Modeling Gamma-Ray Emission From the High-Mass X-Ray Binary LS 5039

Stan Owocki[1†], Atsuo Okazaki[2], and Gustavo Romero[3]

[1]Bartol Research Institute, Department of Physics and Astronomy, University of Delaware, Newark, DE 19716, USA
[2]Faculty of Engineering, Hokkai-Gakuen University, Toyohira-ku, Sapporo 062-8605, Japan
[3]Facultad de Ciencias Astronomicas y Geofısicas, Universidad Nacional de La Plata, Paseo del Bosque, 1900 La Plata, Argentina

A few high-mass X-ray binaries–consisting of an OB star plus compact companion–have been observed by Fermi and ground-based Cerenkov telescopes like High Energy Stereoscopic System (HESS) to be sources of very high energy (VHE; up to 30 TeV) γ-rays. This paper focuses on the prominent γ-ray source, LS 5039, which consists of a massive O6.5V star in a 3.9-day-period, mildly elliptical (e ≈ 0.24) orbit with its companion, assumed here to be an unmagnetized compact object (e.g., black hole). Using three dimensional smoothed particle hydrodynamics simulations of the Bondi-Hoyle accretion of the O-star wind onto the companion, we find that the orbital phase variation of the accretion follows very closely the simple Bondi-Hoyle-Lyttleton (BHL) rate for the local radius and wind speed. Moreover, a simple model, wherein intrinsic emission of γ-rays is assumed to track this accretion rate, reproduces quite well Fermi observations of the phase variation of γ-rays in the energy range 0.1-10 GeV. However for the VHE (0.1-30 TeV) radiation observed by the HESS Cerenkov telescope, it is important to account also for photon-photon interactions between the γ-rays and the stellar optical/UV radiation, which effectively attenuates much of the strong emission near periastron. When this is included, we find that this simple BHL accretion model also quite naturally fits the HESS light curve, thus making it a strong alternative to the pulsar-wind-shock models commonly invoked to explain such VHE γ-ray emission in massive-star binaries.

Keywords: X-rays: binaries, gamma-rays: stars, hydrodynamics

1. INTRODUCTION

Among the most active OB stars are those in high-mass X-ray binary (HMXB) systems, in which interaction of the massive-star wind with a close compact companion–either a neutron star or black hole–produces hard (> 10 keV) X-ray emission with characteristic, regular modulation over the orbital period. In recent years a small subset of such HMXB's have been found also to be γ-ray sources, with energies up to ~10 GeV observed by orbiting γ-ray observatories like Fermi, and very-high-energies (VHE) of over a TeV (10^{12} eV) seen by ground-based Cerenkov telescopes like High Energy Stereoscopic System (HESS),

Very Energetic Radiation Imaging Telescope Array System (VERITAS), and Magic. For the one case, known as B 1259-63, in which observed radio pulses show the companion to be a pulsar, the γ-ray emission seems best explained by a pulsar wind shock (PWS) model, wherein the interaction of the relativistic pulsar wind with the dense wind of the massive-star produces strong shocks that accelerate electrons to VHE, with inverse-Compton scattering of the stellar light by these high-energy electrons then producing VHE γ-rays. For the other γ-ray binaries, pulses have not been detected, and the nature of the companion, and the applicability of the PWS model, are less clear.

An alternative MicroQuasar (MQ) model instead pos-

its that accretion of circumstellar and/or wind material from the massive star onto the companion–assumed now to be either a black hole or a weakly magnetized neutron star–powers a jet of either relativistic protons, which interact with stellar wind protons to produce pions that quickly decay into γ-rays, or relativistic pair plasma, which inverse Compton scatters stellar photons to γ-rays. Okazaki et al. (2011) used smoothed particle hydrodynamics (SPH) simulations to examine both the PWS and MQ models, applying them respectively for two systems,

B 1259-63 and LSI +61 303, in which the massive star is a Be star. In such Be binary systems, the compact companion can interact with the Be star's low-density polar wind, and with the dense equatorial disk that arises from orbital ejection, or decretion, from the rapidly rotating star; modeling both types of interaction is key to understanding their high-energy emission.

In the paper here, we apply the same SPH code to a MQ model for the TeV-binary LS 5039, for which the (non-pulsing) compact companion is in a moderately eccentric (e ~0.24), 3.9-day orbit around a massive, non-Be primary star of spectral type O6.5V (see Table 1 for full parameters). This builds on our previous study (Okazaki et al. 2008b) to account now for wind acceleration, instead of just assuming a constant wind speed. A key result is that the orbital variation of the three dimensional (3-D) SPH accretion rate of the stellar wind flow onto the compact companion follows very closely the analytic Bondi-Hoyle-Lyttleton (BHL) rate that depends on the wind speed and orbital separation at each phase (see right panel of Fig. 1). Assuming the mass accretion translates promptly into jet power and thus γ-ray emission, we then apply this re-
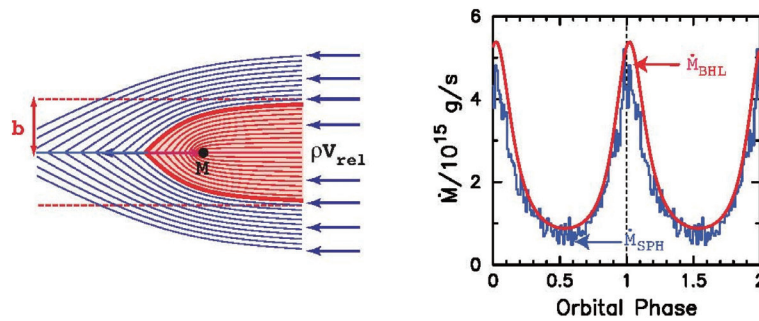
Table 1. Model parameters for LS 5039.

	Primary	Secondary
Spectral type	O6.5V	Compact
Mass (M$_\odot$)	22.9[a]	3.7[a] a
Radius	9.3R$_\odot$ (= 0.31a)	2.5×10^{-3} a
Effective temperature T$_{eff}$ (K)	39,000[a]	–
Wind terminal speed V$_\infty$ (km s^{-1})	2,440	–
Mass loss rate (M$_{sun}$ yr^{-1})	5×10^{-7}[a]	–
Orbital period P$_{orb}$ (d)	3.9060[a]	–
Orbital eccentricity e	0.24[b]	–
Semi-major axis a (cm)	2.17×10^{12}	–

[a]Casares et al. (2005), [b]Szalai et al. (2010).

Fig. 1. Left: illustration of flow streams for simple planar form of Bondi-Hoyle accretion. The gravitational attraction of mass $\dot{M}$ focuses an inflow with relative speed V$_{rel}$ onto the horizontal symmetry axis. This causes material impacting within a Bondi-Hoyle-Lyttleton radius b = 2 GM/V^2 of the axis

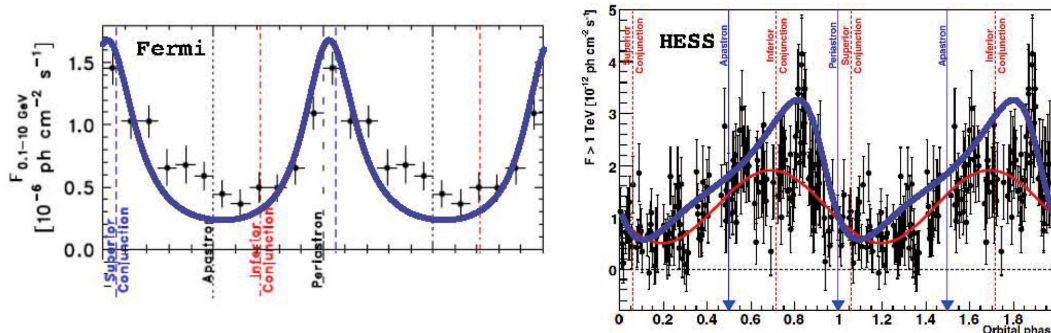

Fig. 2. LS 5039 light curves at energies 0.1-10 GeV observed by Fermi (Abdo et al. 2009, left), and at energies above 1 TeV observed by HESS (Aharonian et al. 2006, right), plotted vs. orbital phase, and compared against the model results based on Bondi-Hoyle-Lyttleton accretion, shown as heavy solid (blue) curves (The light [red] curve represents the best-fit sinusoid for the HESS data).

sult to derive predicted light curves at both the GeV energies observed by Fermi and the TeV energies observed by HESS. For the former, we find that assuming GeV γ-ray emission tracks closely the BHL accretion rate gives directly a quite good fit to the Fermi lightcurve (Abdo et al. 2009, see left panel of Fig. 2 below). But for the latter case one must also account for the attenuation of emitted TeV γ-rays by photon-photon interaction with the optical and UV radiation of the massive star. When this is included, then the predicted TeV lightcurve also closely matches the HESS observations (Aharonian et al. 2006, see right panel of Fig. 2 below).

2. BHL ACCRETION

To provide a physical context for modeling accretion in LS 5039, it is helpful first to review briefly the basic scaling for accretion of an incoming flow onto a gravitating body, as analyzed in pioneering studies by BHL (see Edgar 2004, for references and a modern review). The left panel of Fig. 1 illustrates the basic model. An initially laminar flow with density ρ and relative speed V_{rel} is focused by the gravity of a mass M onto the downstream side of the flow symmetry axis, whereupon the velocity component normal to the axis is cancelled by collisions among the streams from different azimuths. Material with initial impact parameter equal to a critical value b ≡ 2 GM/V² –now typically dubbed the BHL radius, and highlighted by the (red) heavy curve in Fig. 1–arrives on the axis a distance b from the mass, with a parallel flow energy V²/2 just equal to the gravitational binding energy GM/b. Since all material with an impact < b (i.e. within the shaded area) should thus have negative total axial energy, it should be eventually accreted onto the central object. This leads to a simple BHL formula for the expected mass accretion rate,

$$\dot{M}_{BHL} = \rho V_{rel} \pi b^2 = \frac{4\pi\rho G^2 M^2}{V_{rel}^3} \qquad (1)$$

to be accreted onto $\dot{M}$, as outlined here by the bold (red) curve that bounds the lightly shaded region representing accreting material. Right: orbital phase variation of the mass-accretion rate from 3-D SPH simulations (blue), compared to the analytic BHL formula from Eq. (2) (red) assuming the parameters given in Table 1.

In a binary system like LS 5039 there arise additional effects from orbital motion and the associated coriolis terms. But if we ignore these and other complexities, we can use Eq. (1) to estimate how the accretion rate should change as a result of the changes in binary separation r

over the system's elliptical orbit,

$$\dot{M}_{BHL} = \dot{M}_w \frac{G^2 M^2}{r^2 V_w V_{rel}^3} \qquad (2)$$

where $\dot{M}_w \equiv 4\pi r^2 \rho(r) V_w(r)$ is the wind mass loss rate, and $V_{rel}(r)$ is the local magnitude of the relative wind and orbital velocity vectors. We assume here that the stellar wind follows a standard 'beta-type' velocity law, $V_w(r) = V_\infty (1 - R_* / r)^\beta$, where R_* is the O-star radius, V_∞ is the wind terminal speed, and we adopt here a standard velocity power index β = 1.

For the LS 5039 system parameters given in Table 1, the smooth (red) curve in the right panel of Fig. 1 plots the orbital phase variation of this analytically predicted BHL-wind-accretion rate. A principal result of this paper is that this is in remarkably close agreement with the jagged (blue) curve, representing the corresponding accretion rate from full, 3-D SPH simulations, the details of which we discuss next.

3. SPH SIMULATIONS

The SPH code used here is based on a version originally developed by Benz et al. (1990) and Bate et al. (1995), with recent extensions to model interacting binaries by Okazaki et al. (2008a). It uses a variable smoothing length and integrates the SPH equations with the standard cubic-spline kernel using individual time steps for each particle. The artificial viscosity parameters are set to standard values of $\alpha_{SPH} = 1$ and $\beta_{SPH} = 2$. In the implementation here, the O-star wind is modeled by an ensemble of isothermal gas particles of negligible mass, while the compact object is represented by a sink particle of mass M and radius R_{acc} = 5 × 10⁹ cm, i.e. much larger than the ~10⁶ cm radius of a compact object, but still a factor 10 smaller than the minimum (periastron) value of the BHL accretion radius b; if SPH particles fall within this accretion sphere, they are removed from the simulation. The O star's mass exerts a gravitational pull on the binary companion, and the net force of radiative driving vs. gravity of the O-star leads to the outward wind acceleration characterized by the assumed beta = 1 velocity law. In addition, the individual SPH particles feel the gravitational attraction from the compact companion. Finally, to optimize the resolution and computational efficiency of our simulations, the wind particles are ejected only in a narrow range of azimuthal and vertical angles toward the companion; Fig. 1 of Okazaki et al. (2008b) shows that this gives quite similar accretion flow structure to what is obtained in a full,

spherically symmetric model, with however many fewer required particles.

For the system parameters listed in Table 1, Fig. 3 illustrates the nature of the accretion in these SPH simulations, using a time snapshot near periastron, with phase φ = 0.06. The left panel shows the overall, orbitally deflected wind stream that flows radially away from the O-star toward the companion, along with the narrow, dense, gravitationally focused wind-stream in its wake. The right panel zooms in on this wake on a scale within a BHL accretion radius of the companion, as denoted by the dashed white circle arc. The white arrows show that, within the portions of this dense focal stream wake nearest the companion, the flow becomes directed toward the black sphere with assumed accretion radius R_{acc}.

Averaged over some detailed variations, the overall process of accretion in this fully 3-D SPH simulation is thus remarkably similar to the simple laminar flow picture illustrated in the left panel of Fig. 1. The right panel of Fig. 1 shows moreover that the SPH accretion rate–averaged over a phase interval 0.01 to smooth over rapid fluctuations–also agrees remarkably well with the simple BHL rate given by Eq. (2).

4. ACCRETION-POWERED GAMMA-RAY EMISSION

In a microquasar model, the accretion onto the compact companion powers a jet of high-energy protons.

Since the jet acceleration occurs on a scale of a few tens of compact companion radii, it seems reasonable to postulate that jet-wind interaction and the resulting γ-ray emission could promptly track the accretion rate. The left panel of Fig. 2 compares the Fermi lightcurve for LS 5039 at energies 0.1-10 GeV with a simple emission model that scales directly with the BHL accretion rate. The model fits the data quite well, reproducing both the roughly factor five variation range of observed γ-rays, as well as the observed flux peak at a phase very near periastron.[1]

By contrast, the right panel of Fig. 2 shows that the TeV γ-rays observed from LS 5039 by HESS peak well before periastron, toward the phase associated with inferior conjunction, with the flux minimum occurring just after periastron, near the phase for superior conjunction. These phase shifts in the peak and minimum can be explained by accounting for the attenuation of the γ-ray rays through photon-photon interaction with the radiation from the O-star. For TeV γ-rays, the geometric mean of the energies of the γ-rays and stellar UV/optical photons exceeds twice the rest-mass-energy of electrons, thus allowing photon-photon production of electron/positron pairs. The thick (blue) curve in Fig. 2 shows that a simple model combining a BHL-rate emission with such photon-photon attenuation does indeed match the HESS data very well. In contrast, for GeV energy γ-rays the geometric

---

[1]If instead of an eccentricity e = 0.24, we use the larger value e = 0.35 suggested by Casares et al. (2005), the amplitude of orbital variation in mass accretion rate then becomes stronger than this factor five γ-ray variation observed by Fermi.
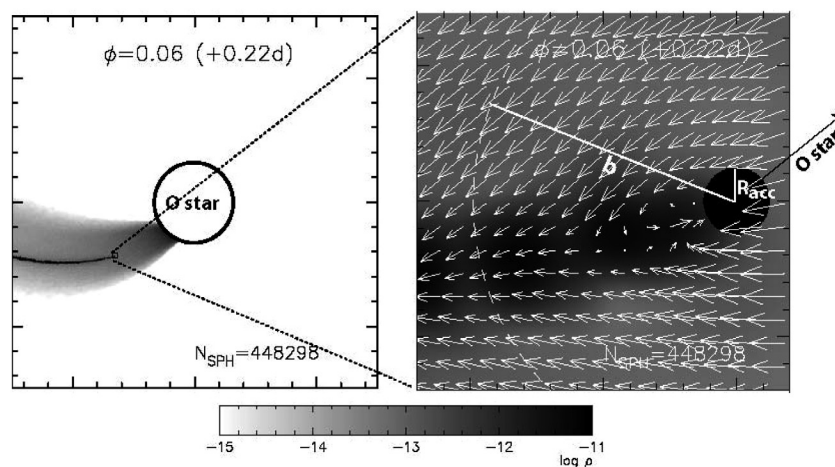

Fig. 3. Snapshots near periastron in smoothed particle hydrodynamics simulation of LS 5039, with the grayscale showing log of the density (in g/cm³), and the arrows denoting flow direction and speed. The left panel gives an overall view of the O-star wind stream in the direction of the orbiting companion, which focuses the impingent wind flow into a narrow, dense, downstream wake. The right panel zooms in on this wake at a much smaller scale, within a Bondi-Hoyle-Lyttleton accretion radius b (marked by the dashed white circle arc) from the companion (represented by the black sphere of assumed accretion radius R_{acc}). The white arrows show how dense material close to the companion and along the gravitational focus axis forms an accretion stream onto the companion, much as in the simple laminar flow picture illustrated in the left panel of Fig. 1.

mean with stellar UV/optical light generally falls below the electron mass-energy, and so the Fermi lightcurve is unaffected by such attenuation.

Since the cross section for photon-photon is highest near the thresh-hold of about ~1 TeV, a pure attenuation model predicts that spectrum should be hardest during the superior conjunction phase of minimum flux and maximum attenuation. However, plots of the photon index for TeV observations by HESS show just the opposite, with the minimum flux corresponding to the softest spectrum. We are currently investigating whether this can be explained by accounting for the progressive softening of γ-rays during a cascade of absorption and reemission associated with pair production and annihilation.

REFERENCES

Abdo AA, Ackermann M, Ajello M, Atwood WB, Axelsson M, et al., Fermi LAT observations of LS 5029, ApJ, 706, L56-L61 (2009). http://dx.doi.org/10.1088/0004-637X/706/1/L56

Aharonian F, Akhperjanian AG, Bazer-Bachi AR, Beilicke M, Benbow W, et al., 3.9 day orbital modulation in the TeV γ-ray flux and spectrum from the X-ray binary LS 5039, A&A, 460, 743-749 (2006). http://dx.doi.org/10.1051/0004-6361:20065940

Bate MR, Bonnell IA, Price NM, Modeling accretion in proto-binary systems, MNRAS, 277, 362-376 (1995).

Benz W, Cameron AGW, Press WH, Bowers RL, Dynamic mass exchange in doubly degenerate binaries. I -0.9 and 1.2 solar mass stars, ApJ, 348, 647-667 (1990). http://dx.doi.org/10.1086/168273

Casares J, Ribó M, Ribas I, Paredes JM, Marti J, et al., A possible black hole in the γ-ray microquasar LS 5039, MNRAS, 364, 899-908 (2005). http://dx.doi.org/10.1111/j.1365-2966.2005.09617.x

Edgar R, A review of Bondi-Hoyle-Lyttleton accretion, NewAR, 48, 843-859 (2004). http://dx.doi.org/10.1016/j.newar.2004.06.001

Okazaki AT, Nagataki S, Naito T, Kawachi A, Hayasaki K, et al., Interaction between the Be star and the compact companion in TeV γ-ray binaries, IAUS, 272, 628-629 (2011). http://dx.doi.org/10.1017/S174392131101163X

Okazaki AT, Owocki SP, Russell CMP, Corcoran MF, Modelling the RXTE light curve of η Carinae from a 3-D SPH simulation of its binary wind collision, MNRAS, 388, L39-L43 (2008a). http://dx.doi.org/10.1111/j.1745-3933.2008.00496.x

Okazaki AT, Romero GE, Owocki SP, The accretion regime of LS 5039: 3-D SPH simulations, in Proceedings of the 7th INTEGRAL Workshop, Copenhagen, Denmark, 8-11 Sep 2008b, PoS(Integral08)074.

Szalai T, Kiss LL, Sarty GE, Looking into the heart of a beast: the black hole binary LS 5039, JPhCS, 218, 012028 (2010). http://dx.doi.org/10.1088/1742-6596/218/1/012028